THE ASTROPHYSICAL JOURNAL, 487:809–817, 1997 October 1

THE RINGS AROUND THE EGG NEBULA

AMOS HARPAZ,[1,2] SAUL RAPPAPORT,[2] AND NOAM SOKER[1]

Received 1997 March 10; accepted 1997 May 15

ABSTRACT

We present an eccentric binary model for the formation of the proto–planetary nebula CRL 2688 (the Egg Nebula) that exhibits multiple concentric shells. Given the apparent regularity of the structure in the Egg Nebula, we postulate that the shells are caused by the periodic passages of a companion star. Such an orbital period would have to lie in the range of 100–500 yr, the apparent time that corresponds to the spacing between the rings. We assume, in this model, that an asymptotic giant branch (AGB) star, which is the origin of the matter within the planetary nebula, loses mass in a spherically symmetric wind. We further suppose that the AGB star has an extended atmosphere (out to ~ 10 stellar radii) in which the outflow speed is less than the escape speed; still farther out, grains form and radiation pressure accelerates the grains along with the trapped gas to the escape speed. Once escape speed has been attained, the presence of a companion star will not significantly affect the trajectories of the matter leaving in the wind and the mass loss will be approximately spherically symmetric. On the other hand, if the companion star is sufficiently close that the Roche lobe of the AGB star moves inside the extended atmosphere, then the slowly moving material will be forced to flow approximately along the critical potential surface (i.e., the Roche lobe) until it flows into the potential lobe of the companion star. Therefore, in our model, the shells are caused by periodic cessations of the isotropic wind rather than by any periodic enhancement in the mass-loss process.

We carry out detailed binary evolution calculations within the context of this scenario, taking into account the nuclear evolution and stellar wind losses of the giant as well as the effects of mass loss and mass transfer on the evolution of the eccentric binary orbit. From the initial binary parameters that we find are required to produce a multiple concentric shell nebula and the known properties of primordial binaries, we conclude that $\sim 0.3\%$ of all planetaries should go through a phase with multiple concentric shells.

Subject headings: binaries: general — ISM: structure — planetary nebulae: general — planetary nebulae: individual (CRL 2688) — stars: AGB and post-AGB — stars: mass loss

1. INTRODUCTION

A planetary nebula (PN) is an extended region of gas surrounding a hot, dense central star. The nebula is expanding, and its average matter density decreases with time. During the PN phase, the central star emits predominantly in the UV range, and this radiation ionizes the nebular matter. Upon recombination, the atoms emit a large fraction of the absorbed energy in lines in the visible band, and this is the emission that is usually observed from such an object. From typical expansion velocities, a lifetime of 10,000–20,000 yr can be estimated for the observed nebulae, after which time the gas is too far from the central star to yield a sufficient surface brightness for detection. At later evolutionary times, all that remains is a cooling white dwarf star.

The inner boundary of most PNs is a "matter" boundary, in that the space inward of this point has a very low density. On the other hand, the outer boundary of many PNs is not limited by nebular material, but is an ionization front whose location is determined by the rate of the ionizing radiation emitted by the central star. In fact, for many PNs, a "halo" of optically nonradiating gas is observable around the fluorescing part of the nebula (Morris 1987; Bowen 1988; Hearn 1990; Vassiliadis & Wood 1993).

The simplest and perhaps most general picture for the creation of a PN is that of an asymptotic giant branch (AGB) star losing mass in the form of a stellar wind at a rate that increases with increasing stellar radius and luminosity. (Since these two properties of the star are increasing functions of its core mass, we can relate the increase of the stellar wind mass-loss rate to the increase of the stellar core.) The matter that leaves the star as a continuous wind forms an expanding gas cloud that spreads to very large distances from the star until it blends into the interstellar medium. This expanding wind is not observed as a luminous nebula as long as the stellar radiation cannot substantially ionize the gas. An expanding cold gas is observed around many AGB stars (Morris 1987; Bowen 1988; Hearn 1990; Vassiliadis & Wood 1993). The velocity of the gas and its density are measured, and the rate of the mass loss from the star can be calculated. According to this picture, the creation of a PN is the last phase in the evolution of AGB stars, during which the progenitor star loses its hydrogen rich envelope via a continuous wind; the matter lost by the wind forms an expanding nebula, whose inner part is ionized by the hot radiation of the remnant central star and forms the luminous PN. The appearance of the PN as a luminous object surrounding the star (i.e., the "birth" of the PN) occurs when the entire envelope of the star has been lost and the bare, hot core of the star has been exposed.

During the first phase of the AGB evolution (when its core mass is 0.5–0.6 $M_\odot$), the mass-loss rate is moderate (10^{-7} to $10^{-6}\ M_\odot\ \mathrm{yr}^{-1}$), and increases with increasing core mass. Toward the later phases, this rate increases significantly, probably by another factor of 10 or more to values of $10^{-5}\ M_\odot\ \mathrm{yr}^{-1}$ and higher, over a relatively short time-

[1] Department of Physics, University of Haifa at Oranim, Tivon 36006, ISRAEL; PHR 89AH@vmsa.technion.ac.il; soker@physics.technion.ac.il.
[2] Physics Department, Massachusetts Institute of Technology, Cambridge, MA 02139; sar@mit.edu

scale (Renzini 1981; Iben & Renzini 1983; Wood 1986). This phase of dramatically increased rate is called the "superwind;" the wind velocity in this phase is similar to that of the moderate (regular) wind, but the mass-loss rate is much larger. When most of the stellar envelope is consumed via this superwind and the hot core is exposed, a "fast" wind results owing to low-density matter accelerated by the radiation pressure of the hot central star (Kwok, Purton, & FitzGerald 1978). The velocity of the fast wind is high (~ 2000 km s^{-1}), but the mass-loss rate is relatively low. The interaction of the fast wind with the matter that was last to leave the star through the regular wind or the superwind results in a double shock wave, with a contact discontinuity between the two shocks. The contact discontinuity forms the inner boundary of the PN (interacting winds model; Kwok et al. 1978).

During the past two decades, much effort has been invested in trying to understand how the stellar wind is created. Several mechanisms have been suggested, but none of them has been found satisfactory. Although the exact mass-loss process from an AGB star is not completely understood, it is commonly assumed that radiation pressure on dust grains causes the high mass-loss rate (Knapp & Morris 1985). The dust grains form at low temperatures (~ 1200 K), while the effective temperature of the star is ~ 3000 K. The grain formation zone should thus be far from the stellar surface. The common picture (Morris 1987; Bowen 1988; Hearn 1990; Vassiliadis & Wood 1993) is that there exists a region between the stellar surface and the grain formation zone in which matter moves with low velocities (lower than the escape speed) and the final acceleration, which imparts velocities above the escape speed, takes place at the grain formation zone. Johnson, Alexander, & Bowen (1995) show that adding radiative acceleration to molecules in the extended atmosphere models of Mira variables can further increase the mass-loss rate. In all these models, the mass loss is effectively a continuous process.

The late AGB evolutionary phase of a star is also characterized by (1) stellar pulsations of the kind called "Mira" pulsations, whose period is one to a few years; and (2) "thermal pulses," which are nuclear flashes in the helium-burning shell, whose timescale is typically hundreds of thousands of years (Vassiliadis & Wood 1993). Certainly, such events do change the mass-loss rate but on timescales that are entirely different from that of PN formation. In general, the mass loss that forms PNs is a continuous process.

To this point, we have been describing a single-star formation scenario for PNs. PNs created through such scenarios should, in principle, exhibit and maintain spherical symmetry. However, most stars in the Galaxy reside in multistellar systems, and, therefore, one can expect that a large fraction of PNs will form in binary systems and will be influenced by the presence of the companion star (Yungelson, Tutukov, & Livio 1993). Such PNs would be expected to exhibit nonsymmetric properties. The nonspherical nebulae are classified into two major groups: elliptical and bipolar (also called "butterfly" or "bilobal") PNs (see Stanghellini 1995 for a review). Other axisymmetrical features, such as jets, allow subclassifications within these groups.

It has been known for a long time that, in fact, when examined in detail, most PNs have nonspherical structures. However, the question of whether nonspherical PNs can be formed through single-star evolution or whether a binary companion is necessary has still not been resolved, despite having been debated for two decades (see, e.g., Fabian & Hansen 1979; Livio 1982; Livio, Salzman, & Shaviv 1979; Morris 1981; Webbink 1979a). In recent years, the binary model has been studied in more detail than has the single-star evolutionary model (the supporting evidence for the binary models, including substellar companions, is summarized by Soker 1997). Soker (1997) estimates that 5%–15% of all PNs are truly spherical, namely, their progenitors did not interact with a companion, and these PNs were formed through single-star evolution. Some 30% of PNs show strong spatial asymmetries that are clearly the result of an interaction with a stellar companion. Perhaps $\frac{2}{3}$ of these underwent a common-envelope phase in which the companion star spiraled into and ejected the envelope of the AGB star (see, e.g., Yungelson et al. 1993); a substantial fraction of these will result in close binary nuclei. The remaining one-third of these interacted with a binary stellar companion but managed to avoid a common envelope phase; these form mainly bipolar PNs (Corradi 1995; Corradi & Schwarz 1995; Schwarz & Corradi 1995; Stanghellini 1995). Similar estimates for PNs formed by strong interactions with stellar companions were obtained by Han, Podsiadlowski, & Eggleton (1995) in their Monte Carlo simulations. The remaining $\sim 60\%$ of PNs show weaker signs of nonsphericity, and Soker (1997) estimates that these were very likely influenced by less massive companions, such as brown dwarfs or planets.

We note that the list of PNs found to have close-binary nuclei (Bond & Livio 1990) and the list of 43 bipolar PNs of Schwarz & Corradi (1995; also in Corradi & Schwarz 1995) have only one object in common (NGC 2346). Therefore, PNs that are formed from binary systems that evolve through a common envelope are more likely to result in an elliptical morphology (see Bond & Livio 1990) than are the bipolar PNs studied by Schwarz & Corradi (1995). In the latter case, when the companion avoids a common envelope phase, it may accrete mass at high rates from the AGB star (see, e.g., Morris 1987; Soker & Livio 1994). If this transfer rate is higher than that which the companion star can accommodate, it is likely to result in the formation of a massive accretion disk. It is then speculated that the excess mass that cannot be accreted onto the companion is ejected in the form of jets in the polar directions (Soker & Livio 1994). The similar morphology of bipolar PNs and symbiotic nebulae provides strong support for this model of the formation of bipolar PNs (Corradi & Schwarz 1995; Schwarz & Corradi 1995).

Thus we see that most planetary nebulae exhibiting strong asymmetries were probably formed in binary systems. The orbital periods of systems undergoing the types of interactions described above probably do not exceed a few years. However, as we shall demonstrate, this does not preclude significant effects on the formation of PNs by companions in much wider orbits.

In the present paper, we study the effect of wide ($P_{\rm orb} \sim 100$ yr), eccentric binary companions to AGB stars on the mass-loss process and the morphology of the resultant PN. In particular, we present a model for the fascinating concentric ring structure observed in the Egg Nebula (Sahai, Trauger, & Evans 1995). Some background information on the Egg Nebula is presented in § 2. The basic model for the formation of shell-like features in PNs is described in § 3. In

this model, it is the periodic passages of a companion star that affect the normal stellar wind outflow of matter from the AGB star. For some portion of each orbit, the proximity of the companion diverts the wind from its isotropic configuration to be directed in the orbital plane of the binary. These diversions create periodic *gaps* in the mass flow toward the polar directions that we see as multiple, shell-like structures. The effects of mass loss and mass transfer in the progenitor binary are discussed in § 4. Our exploratory calculations of binary evolution with periodic incursions of the Roche lobe into the extended envelope of the AGB star and the formation of shell-like structure are presented in § 5. For some illustrative system parameters, we follow the detailed evolution of both the mass-losing giant and the binary orbit during the loss of the entire envelope of the giant. We find that the semimajor axis and the eccentricity of the orbit typically grow during the evolution; however, the size of the critical potential lobe near periastron remains nearly constant. Our results are summarized in § 6. We conclude that the model can successfully reproduce the features observed as shells of matter, with spacings of a few hundred years between them.

2. THE EGG NEBULA

The Egg Nebula (CRL 2688) is a bipolar nebula located at a distance of about 1 kpc with an angular diameter of $\sim 30''$. It is most likely a protoplanetary nebula, which is a PN in its final phase of formation. Its central star is not observed, as it is embedded in a thick dust shell that is possibly being ejected by the superwind from the star. The velocity measured for the expanding envelope is 19.7 ± 0.3 km s^{-1}, while the mass ejection rate is inferred to be about $1.3 \times 10^{-4}\ M_\odot\ \mathrm{yr}^{-1}$ (Knapp & Morris 1985). The latest *Hubble Space Telescope* images (Sahai & Trauger 1996) give the overall impression of a nebula that consists of a large number (~ 20) of concentric shells, with a roughly uniform spacing of $0''.5$, or ~ 0.003 pc. For typical outflow speeds of ~ 20 km s^{-1}, this implies a temporal spacing of about 200 yr between the rings. The nebula is also characterized by a large obscured region, probably due to dust, which appears in its central midplane (Latter et al. 1993). In addition, there are prominent, opposing "jetlike" features (or remnants thereof) that appear to lie on the surface of, or perhaps to form, a cone.

We also note that CRL 2688 is a reflection nebula, which means that the gas in the nebula is not substantially ionized, its temperature is low, and dynamical effects due to pressure gradients can be ignored. This set of conditions allows the ring structure to remain stable for a substantial interval of time. As the envelope of the central stellar object shrinks during the course of its evolution and the effective temperature grows, the surrounding nebular gas will become both heated and ionized, and pressure imbalance between regions with different densities will cause the ring structure to be smeared out.

Detailed observations of CRL 2688 (the Egg Nebula; Latter et al. 1993) have been carried out in the near-infrared, both in lines (mainly H_2 emission) and in the continuum (from dust). These lines are present in the bipolar lobes as well as in an equatorial torus, which extends around the central region of the object to a distance of 0.02 pc. The density of the dust decreases with increasing angular distance from the equatorial region, with very little dust near the poles. It is likely that the dust grains are large graphite particles (Latter et al. 1993).

3. THE BASIC MODEL

The apparent shell-like structure in the Egg Nebula has led us to speculate that its appearance may be related to relatively close, periodic passages of a binary companion to the progenitor AGB star during the formation of the nebula. Before proceeding with a description of our model, we acknowledge two other obvious, different possibilities for the formation of multiple shell-like structures in PNs. First, the shells might represent mass ejection episodes triggered by some unknown mechanism in an isolated star (see, e.g., Tuchman 1991). Second, Deguchi (1997) suggests that the rings of the Egg Nebula are the result of instabilities in the flow of the dust relative to the gas in an otherwise continuous mass-loss process.

Given the apparent regularity of the shell structure in the Egg Nebula, we postulate that the underlying "clock" in the system is the orbital period of a companion star. Such an orbital period would have to lie in the range of 100–500 yr, the approximate timescale that corresponds to the spacing between the rings. The range of possible values reflects the uncertainties in the distance to the Egg Nebula, the outflow velocity of the nebular material, and the average angular separation between the rings.

We assume, in this model, that the AGB star, which is the origin of the matter within the planetary nebula, loses mass in a spherically symmetric wind during times when the companion is farthest away in its eccentric orbit, but that this mass loss is diverted in the direction of the companion star when the distance closes. We further suppose that the AGB star has an extended atmosphere (out to ~ 10 stellar radii; see the discussion below) in which the outflow speed is less than the escape speed from the AGB star. It is thought that the matter in the extended atmosphere attains escape speed at about the radial distance where grains form, and it is the radiation pressure that accelerates the grains (Morris 1987; Bowen 1988; Hearn 1990; Vassiliadis & Wood 1993). The momentum acquired by the grains is transferred to the entrained gas by the strong coupling between the grains and the gas (Gilman 1972). Once escape speed has been attained, the presence of a companion star will not significantly affect the trajectories of the matter leaving in the wind, and the mass loss will be approximately spherically symmetric. On the other hand, if the companion star is sufficiently close that the Roche lobe of the AGB star moves inside its own extended atmosphere (i.e., the radius where grains form), then the slowly moving material will be forced to flow approximately along the critical potential surface (i.e., the Roche lobe) until it flows into the potential lobe of the companion star. Therefore, in our model, the rings are caused by periodic cessations of the isotropic wind rather than by any enhancement in the mass-loss process.

AGB stars have very tenuous outer envelopes, with densities dropping to as low as 10^{-10} g cm^{-3} at the photosphere. Such stars are apparently capable of generating large stellar winds with a mass-loss rate given approximately by the Reimers (1975) formula

$$\dot{m} = \eta(4 \times 10^{-13}) \frac{LR}{M}\ M_\odot\ \mathrm{yr}^{-1}\ , \qquad (1)$$

where L, R, and M are the stellar luminosity, radius, and

mass, respectively (given in solar units), and η is a constant of order unity. For highly evolved AGB stars, this rate can be as high as $10^{-5} M_\odot$ yr^{-1}; in this case, the value of η must be approximately an order of magnitude larger. The dust grains mentioned above are supposed to form relatively far from the AGB star (at, e.g., $\sim$5–20 stellar radii), where the temperature in the slowly moving wind has fallen below that required for grain formation. It is the matter in the region between the photosphere and the grain-forming region that contains the slowly moving outflow of matter that we refer to as the "extended atmosphere" of the star.

Models for this region of an AGB star's atmosphere are poorly understood (Morris 1987; Hearn 1990; Bowen 1988; Vassiliadis & Wood 1993), but we make four simplifying assumptions for obtaining the properties of such an hypothesized extended atmosphere. These are as follows: (1) the density falls off as r^{-2} (i.e., the material has a constant outflow speed); (2) the optical depth through this extended atmosphere is required to be substantially less than unity, so that it does not conceal the photosphere and such that it would *not* be easily detectable observationally; (3) the temperature is linearly interpolated (with radius) between the effective temperature, T_e, and $T \simeq 1200$ K at the outer boundary (where grains are supposed to form); and (4) matter continues to flow into the extended atmosphere at the same rate, on average, as the nominal rate at which it leaves in the stellar wind, even if the grain-forming region is temporarily destroyed. Only the last of these assumptions is actually important for the model we present here.

The density profile of the extended atmosphere used for our models is shown in Figure 1, joined with the density profile of the AGB star itself. The optical depths were computed with the Alexander (1975) opacities. The mass of the AGB star at this point in its evolution is 0.9 $M_\odot$, and its core mass is 0.7 $M_\odot$, while the amount of mass contained in the extended atmosphere is only 0.007 $M_\odot$. Note that the material above the photosphere (see Fig. 1) extends out to $\sim$10 times the stellar radius, at which point grains are assumed to be formed and a higher velocity wind of much lower density commences. The outflow velocity that corresponds to the densities in the extended atmosphere in Figure 1, and which yields the same mass-loss rate as that of the superwind ($\sim 10^{-4} M_\odot$ yr^{-1}), is about 1.2 km s^{-1}. The optical depth of the extended atmosphere in this particular

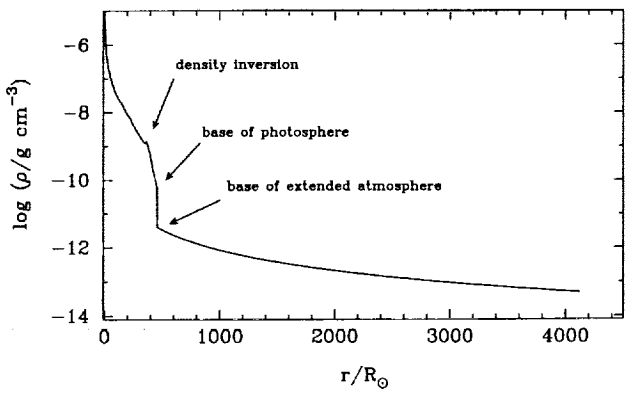

FIG. 1.—Density profile of an AGB star and its hypothesized extended envelope. Densities exceeding 10^{-5} g cm^{-3} are found only inward of $\sim 3\ R_\odot$ and are not shown on the plot. At this phase of its evolution, the AGB star has a mass of 0.9 $M_\odot$, its core mass is 0.7 $M_\odot$, and the total integrated mass in the extended envelope is $\sim$0.007 $M_\odot$. Several benchmark features in the atmosphere are indicated with arrows.

model is $\sim$0.035. We do not propose a self-consistent hydrodynamic treatment of such a slowly expanding extended atmosphere in this paper; we merely postulate that it can exist and that it cannot be ruled out at the present time by observational constraints.

Our approach in this paper is to evolve binary systems from their original state, through the red giant and AGB phases of the primary, until the envelope has been completely lost. While following the evolution of the primary, including mass loss in a stellar wind, we also follow the evolution of the binary orbit, taking into account the effects of the mass loss and transfer on the semimajor axis and the eccentricity. The evolution of the primary is followed with a combination of a Henyey-type code and some simplified models, which we discuss below.

4. EFFECTS OF MASS LOSS AND TRANSFER ON THE BINARY ORBIT

When the primordial binary starts to evolve, the primary is much smaller than its Roche lobe. The primary, which by definition initially has the higher mass, evolves faster than the secondary star. We begin our evolution calculations when the primary is already on the first giant branch (FGB) (with a core mass of $\sim$0.35 $M_\odot$) and the masses of the two stars have become nearly equal owing to wind mass losses by the primary star. We assume that the secondary at this point is still on the main sequence. As the primary first ascends the red giant branch and then becomes an AGB star, its size and stellar wind mass-loss rate both grow as a very large power of its core mass.

Before the AGB primary and its extended atmosphere begin to approach the critical potential lobe, the mass loss in the stellar wind is taken to be isotropic. For the case of isotropic mass loss, we utilize prescriptions given by Eggleton (1997) to evolve both the eccentricity, e, and the semimajor axis, a, of the binary. The specific expressions we used are

$$\frac{\delta a}{a} = \frac{|\delta m_w|}{M} \frac{(1 + 2e\cos\theta + e^2)}{(1 - e^2)}, \tag{2a}$$

$$\delta e = \frac{|\delta m_w|}{M} (e + \cos\theta), \tag{2b}$$

where δm_w is the mass lost from the binary in the stellar wind, M is the total mass of the system, e is the orbital eccentricity, and θ is the polar angle of the position vector from the center of mass to the secondary ($\theta = 0^o$ corresponds to the time of periastron passage). Using the relation $dt = d\theta \Omega_K^{-1}(1 - e^2)^{3/2}(1 + e\cos\theta)^{-2}$, where dt is the time interval during which the orbit advances by an angle $d\theta$ and Ω_K is the Kepler frequency, it is straightforward to show that equation (2b), when averaged in time over a complete orbit, yields 0 (under the assumption that the wind mass-loss rate is constant in time). Thus, during this phase of the evolution (i.e., isotropic mass loss through a stellar wind only), the semimajor axis grows while the eccentricity remains constant.

At some point during the evolution, the outer boundary of the extended atmosphere of the AGB star begins to come into contact with its Roche lobe for at least some portion of the orbital period. As the AGB star grows, the duration of this contact increases. As mentioned above, we assume that even during intervals when the Roche lobe is inside the

outer boundary of the extended atmosphere (assumed to be ~ 9 times the radius of the AGB star), the mass-loss rate from the AGB star remains the same as it was before the incursion but that the slower moving matter is directed toward, and captured by, the companion star. We also compute the effects on the orbital parameters of mass transfer during these epochs, the prescriptions for which were also taken from Eggleton (1997):

$$\frac{\delta a}{a} = 2\,|\,\delta m_{\rm tran}\,|\left(\frac{1}{m_g} - \frac{1}{m_s}\right)\frac{(1 + 2e\cos\theta + e^2)}{(1 - e^2)}\,, \quad \text{(3a)}$$

$$\delta e = 2\,|\,\delta m_{\rm tran}\,|\left(\frac{1}{m_g} - \frac{1}{m_s}\right)(e + \cos\theta)\,, \quad \text{(3b)}$$

where $\delta m_{\rm tran}$ refers to the mass that is transferred and m_g and m_s are the masses of the primary (AGB star) and secondary (companion) star (recall that $m_g < m_s$). For now, we assume that all the mass lost during these epochs is transferred to, and captured by, the secondary.

In general, the standard Roche lobe formalism cannot be applied to eccentric orbits since the AGB star will not be corotating with the orbit at any time (except for two possible instants) during the orbit. There is a specific formulation for computing the approximate equipotential surfaces at any point in an eccentric orbit (Avni 1976); however, the other uncertainties in the current model do not warrant such an elaborate treatment. Instead, we simply take the radius of the critical potential lobe of the AGB star to be

$$R_L \simeq 0.46D\left(\frac{m_g}{M}\right)^{1/3}\,, \quad \text{(4)}$$

where D is the instantaneous orbital separation between the two stars (Kopal 1959; Paczyński 1967a). Here we have utilized a standard fitting formula for the radius of the Roche lobe, but the radius of a circular orbit has been replaced by the instantaneous separation in an eccentric orbit.

5. EVOLUTION OF THE AGB STAR AND FORMATION OF THE PLANETARY NEBULA

Early in the binary evolution, before Roche lobe contact with the AGB extended atmosphere is made, the evolution of the primary is carried out via a technique developed by Webbink, Rappaport, & Savonije (1983), Joss, Rappaport, & Lewis (1987), and Rappaport et al. (1995). In this approach, the properties of the low-mass giant are taken to be nearly unique functions of its core mass (see also Refsdal & Weigert 1970, 1971). In this case, the core mass–radius and core mass–luminosity relations form a closed set of equations that allow the evolution of the donor star to be followed very quickly. The core mass–radius relation derived by Rappaport et al. (1995) holds for a wide range of core masses from 0.15 $M_\odot$ to $> 1\ M_\odot$ and is given by

$$R_g \simeq 4590\left(\frac{m_c^{4.5}}{1 + 4m_c^4}\right) + R_{\rm ms}\,, \quad \text{(5)}$$

where m_c is the core mass of the giant (cf. Eggleton 1997; P. Eggleton 1992, private communication), and $R_{\rm ms}$ is the radius of a star of mass m_g when it is on the main sequence. This relation resulted from a fit to models that spanned a wide range of chemical compositions and envelope masses for the giant (on both the FGB and the AGB), as well as a range of mixing-length parameters (Rappaport et al. 1995). Thus, this core mass-radius relation is especially useful if the detailed prior history of the giant is unknown. The complementary expression for the core mass–luminosity relation was taken from P. Eggleton (1992, private communication):

$$L_g \simeq \frac{10^{5.3}m_c^6}{1 + 10^{0.4}m_c^4 + 10^{0.5}m_c^5} + L_{\rm ms} \quad \text{(6)}$$

(see also Eggleton 1966; Paczyński 1970; Refsdal & Weigert 1970), where $L_{\rm ms}$ is the luminosity of a star of mass, m_g, when it is on the main sequence. Evolutionary calculations based on equations (5) and (6) do not incorporate special events during the stellar evolution, such as the helium flash in the core at the tip of the first red giant branch and the helium shell flashes (thermal pulses) during the AGB evolution. They do not cover the evolution along the horizontal branch as well. However, they do yield an adequate overall representation of the evolution of the star.

The stellar radius as given by equation (5) is correct during most of the stellar evolution, except for the final AGB phase, when the stellar envelope falls below $\sim 0.1\ M_\odot$, at which point the stellar radius begins to *shrink* with further loss of mass from the envelope. We have carried out detailed evolutionary calculations with a full Henyey code for two stellar models of AGB stars to explore this effect: these were for core masses of 0.6 and 0.7 $M_\odot$, with envelope masses starting at 0.2 $M_\odot$. We were particularly interested in following the evolution of the stellar radius as a function of the envelope mass during the final stage of loss of the stellar envelope and found that during these final stages, the stellar luminosities remain nearly constant, even while the radius *decreases*. Based on these calculations, we devised a fitting formula for the stellar radius as a function of the envelope mass, $m_{\rm env}$, during the final stage of mass loss. The expression for $R_g(m_{\rm env})$ is given by

$$R_g = R_0\left(\frac{m_{\rm env}}{0.1\ M_\odot}\right)^{0.125} \quad \text{for } m_{\rm env} < 0.1\ M_\odot\,, \quad \text{(7)}$$

where $R_0 = 450\ R_\odot$ in our calculations. This formula was used instead of equation (5) when the envelope mass of the giant decreased below 0.1 $M_\odot$.

At each stage in the computed evolution of the primary, its radius and luminosity are known, so that its wind mass-loss rate can be computed via the Reimers formula (eq. [1]). The envelope mass continues to decrease throughout the evolution because of losses in the stellar wind and by nuclear burning, which adds mass to the core of the giant. For the regular wind mass-loss rate, we used the Reimers formula, with $\eta = 0.6$. In order to account for the superwind (Renzini 1981; Iben & Renzini 1983; Wood 1986) that occurs late in the AGB evolution, η was, somewhat arbitrarily, increased by a factor of 10 (i.e., $\eta = 6$) when the stellar envelope dropped below 0.25 $M_\odot$.

Using the above prescription for stellar evolution, mass loss/transfer, and binary evolution, we have calculated evolutionary sequences for a range of initial values of the binary system parameters: a_i, m_i, e_i, and so forth. The evolution was continued until the envelope mass was exhausted or the Roche lobe of the AGB star made contact with the extended envelope. If the former case occurred first, the evolution was "unsuccessful" and a new evolutionary run was started. If Roche lobe contact was made while the

envelope of the AGB star still had mass left in it, the final stage of evolution was followed to produce a nebula with shell-like structure.

As an example of the evolution of a typical system that might produce a nebula consisting of concentric shells, we have chosen the following illustrative set of binary system parameters to start our evolutionary calculations: $m_g = 1.93\ M_\odot$, $m_c = 0.35 M_\odot$, $m_s = 1.93 M_\odot$, $e = 0.3$, and $P_{orb} = 80$ yr. The evolutionary calculations are shown in Figure 2 with the evolution of the system parameters displayed in two ways: first (Fig. 2*a*), as functions of the log of the evolution time (where the zero point is taken to be the end of the evolution), second (Fig. 2*b*), as functions of time (on a linear scale) for only the final 6500 yr of the evolution. As indicated above, the evolutionary calculations began at the point where the two stars in the system had equal masses and the core mass of the giant star had already reached 0.35 $M_\odot$; however, since the *initial* mass of the giant star was higher than that of its companion, it reached the AGB phase while the secondary was still a main-sequence star.

The bottom panel in Figure 2 displays the stellar mass (*solid line*) and the core mass (*dashed line*); one can clearly see that the envelope is consumed principally by the wind mass loss, while the amount of mass processed by nuclear reactions and added to the core is modest by comparison. The second panel from the bottom shows the evolution of the stellar radius, and we see both the initial growth in the radius of the AGB star and its subsequent decline toward the end of the evolution. In these evolutionary calculations, we assumed that the radius of the extended atmosphere is always 9 stellar radii in size during the entire time that the stellar radius is increasing. When the stellar radius begins to shrink, we assume that the radius of the extended atmosphere retains its maximum value.

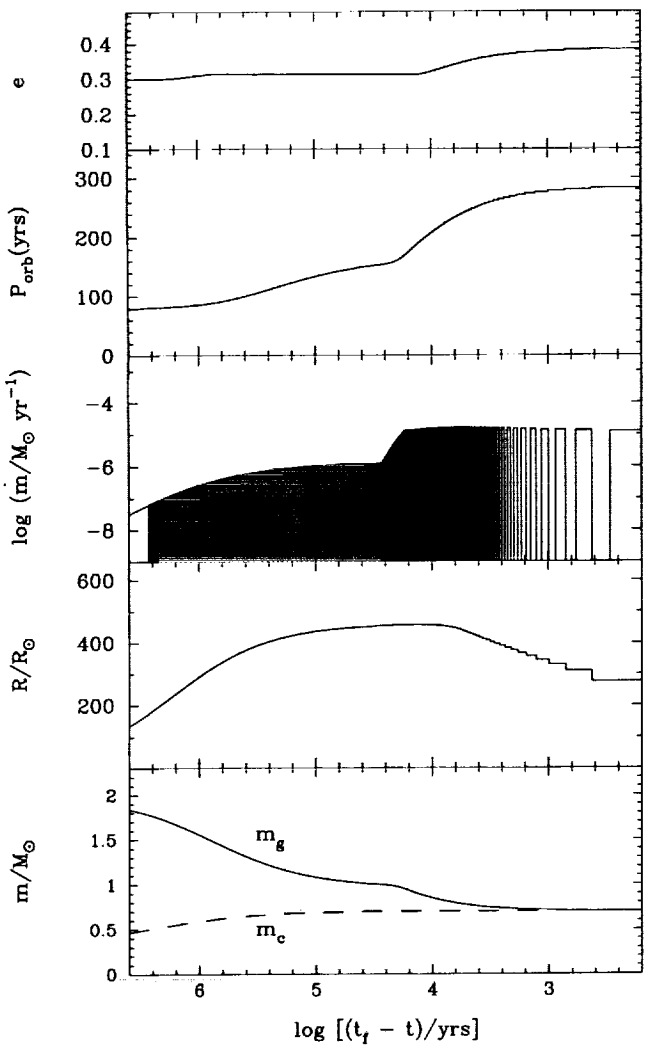

FIG. 2*a*

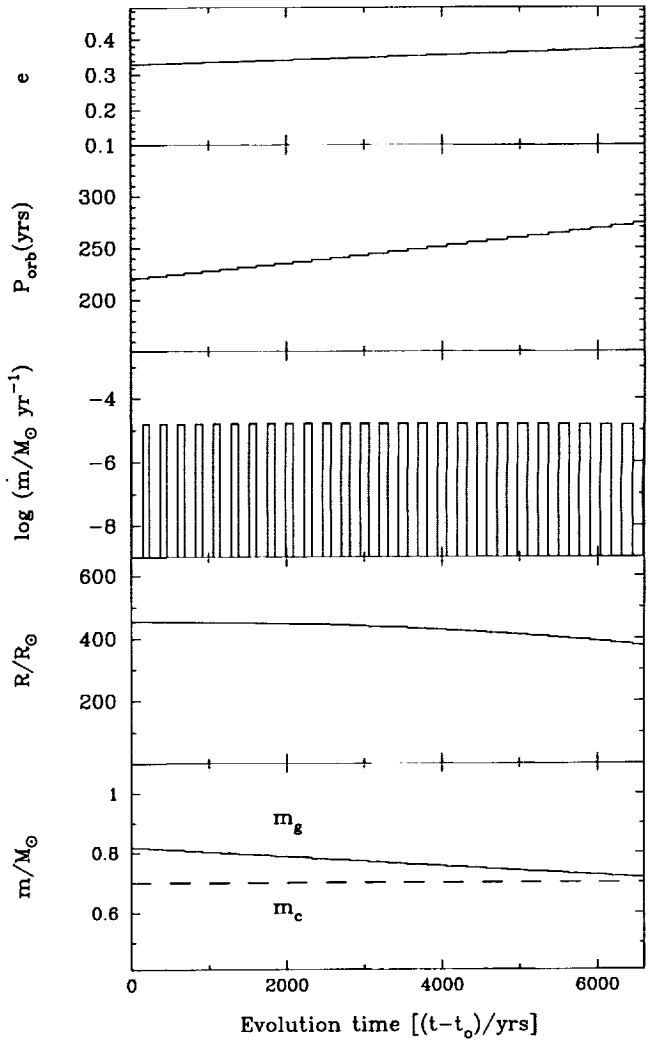

FIG. 2*b*

FIG. 2.—Illustrative binary evolution leading to the production of a concentric-shell planetary nebula. The evolution of various system parameters are shown as a function of log $(t_f - t)$ in (*a*) and as a function of $t - t_0$ for 6500 yr toward the end of the evolution in (*b*); in this notation, t is the time from the start of our binary evolution calculation, while t_f is the evolution time when the calculations were terminated ($t_0 = 1.5 \times 10^7$ yr and $t_f = t_0 + 8000$ yr). Parameters shown include (*top to bottom*) orbital eccentricity, orbital period, mass-loss rate that goes into the isotropic stellar wind, the stellar radius of the giant, and the mass and the core mass of the giant star. The evolution shown in this figure includes only the evolution along the AGB phase. The lightly shaded region in the middle of panel (*a*) denotes times when the ordinary stellar wind is periodically modulated by the companion star but where there is insufficient resolution on the plot to show the modulation. The heavily shaded region is the same, except during the superwind phase.

The middle panel in Figure 2 shows the rate of mass loss that goes into the isotropic stellar wind. As explained earlier, we assumed that the mass loss from the AGB star was continuous, but during the incursion of the Roche lobe into the extended atmosphere of the AGB star, the mass loss was diverted from its normal isotropic distribution to the equatorial plane. The spacings in the figure *between* the high values of the mass-loss rates represent the intervals during which the mass was diverted from the isotropic wind. It is these times that should have a one-to-one correspondence with the less dense regions between the shells in the Egg Nebula.

The top two panels in Figure 2 display the evolution of the orbital period and eccentricity. The periods were calculated from the semimajor axis, a, whose evolution in turn was calculated according to equations (2a) and (3a), while the eccentricity was evolved according to equations (2b) and (3b). As was noted above, both equations (2b) and (3b) average to zero over a complete orbital period for the case of pure isotropic wind loss, or pure Roche lobe transfer. In most cases, however, the Roche lobe enters the extended envelope for only a portion of the orbit. Therefore, equations (2a) and (2b) were integrated numerically along those parts of the orbit when the Roche lobe was outside the extended envelope, while equations (3a) and (3b) were integrated numerically during intervals when the Roche lobe penetrated the extended envelope.

The evolution of the AGB star and the binary orbit as well as the formation of the planetary nebula shells (Fig. 2) divides naturally into three phases. For the first few tens of millions of years, the primary evolves up the giant and AGB branches as if it were an isolated star. When the core mass and radius reach values of $\sim 0.5\ M_\odot$ and $200\ R_\odot$, respectively, the Roche lobe of the AGB star begins to make periodic incursions into its extended atmosphere. In the second phase, which lasts for some 2×10^6 yr, the AGB star grows to $400\ R_\odot$, and it loses nearly $1\ M_\odot$ in a stellar wind. The direction of this wind is modulated by the periodic approach and recession of the companion star; however, the material lost during this second phase expands too far from the AGB star to be illuminated later during the planetary nebula phase. In the final phase, which lasts for some 10^4 yr, a superwind turns on and removes the final $\sim 0.25\ M_\odot$ of the envelope of the AGB star. During this phase there are some 30 episodes where the companion star deflects mass into the equatorial plane; these result in the formation of the ring structure that is seen at the current epoch. Note that during the final 10^4 yr of the evolution, the orbital period increases from ~ 200 to ~ 280 yr, while the eccentricity increases from 0.3 to ~ 0.38. In this regard, we note that tidal friction is unlikely to play a significant role in *reducing* the orbital eccentricity. Here we have utilized an expression for tidal circularization appropriate for low-mass giants given by Zahn (1977, 1989) and Verbunt & Phinney (1995) and find that the circularization timescales exceed 10^8 yr during the entire evolution shown in Figure 2. We also note that there may be some small tidal effects due to the extended atmosphere, but we have assumed these to be negligible.

The evolutionary results shown in Figure 2 and the specific numbers cited above are illustrative only and would change somewhat for different choices of the parameters for the progenitor primordial binary. We have also identified other combinations of orbital periods and eccentricity that could lead to the production of a PN with multiple concentric shells. We show in Figure 3 the orbital period that is required for the Roche lobe to spend 50% of the orbital period within the extended atmosphere of the AGB star as a function of the core mass of the star. This relation is shown for five different assumed orbital eccentricities. To generate these curves, we took $m_s = 2\ M_\odot$ and $m_g = m_c + 0.2\ M_\odot$ (the latter value being appropriate to the onset of the superwind) and assumed that the radial extent of the extended atmosphere was equal to 9 times the radius of the AGB star. As can be seen in Figure 3, shell structure of the type observed in the Egg Nebula would likely be formed for binary systems that have orbital periods in the range of $\sim$ 50–300 yr at the time when the superwind commences; for shorter orbital periods, the shell structure might not be resolvable. Since the orbit tends to grow by about a factor of 2 (in period) between the first contact of the Roche lobe with the extended atmosphere and the onset of the superwind, systems with initial orbital periods in the range of $\sim$25 to 150 yr would be good candidates to form nebular concentric-ring structures. Moreover, orbital eccentricities in the range of $\sim$0.2–0.6 are required to yield a substantial modulation factor in the density profile through the shells. Smaller eccentricities yield too small a duty-cycle for matter going into the shells, while larger eccentricities result in the reverse situation. Finally, the initial mass ratio of the binary, $q = m_s/m_g$, should lie in the range of $\sim$0.8–1.0 in order for the primary to be able to lose enough mass in a stellar wind to make $q > 1$ before contact of the Roche lobe with the extended atmosphere. This is necessary in order for the binary orbit to expand with the subsequent mass trans-

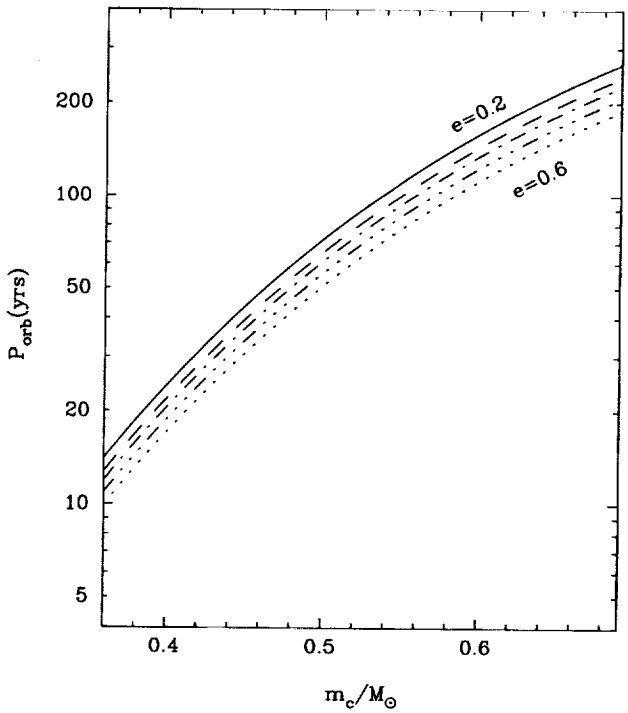

FIG. 3.—Orbital period required for the Roche lobe to be within the extended atmosphere of the AGB star for more than 50% of the orbit as a function of the core mass, m_c, for five values of the orbital eccentricity. The extended atmosphere was assumed to have a radius of ~ 9 times the photospheric radius of the AGB star, and the constituent binary masses were arbitrarily taken to be $m_s = 2\ M_\odot$ and $m_g = m_c + 0.2\ M_\odot$.

fer instead of shrinking (see eq. [3a]). In the case of orbital shrinkage with mass transfer, the Roche lobe would tend to come into direct contact with the photosphere of the AGB star, possibly leading to a mass transfer instability on a dynamical timescale (see, e.g., Paczyński 1967b; Kippenhahn, Kohl & Weigert 1967; Webbink 1979b, 1992).

We can make a rough estimate of the fraction of primordial binaries with the requisite properties described above. The orbital period distribution is approximately uniform in $\log (P_{\rm orb})$ over the period range ~ 1 day to $\sim 10^6$ yr (see, e.g., Abt & Levy 1978; Duquennoy & Mayor 1991). Thus, about 10% of all binaries have initial orbital periods in approximately the correct range. If we assume that the orbital eccentricities of primordial binaries are distributed uniformly in e, then approximately 40% of primordial binaries can be expected to have reasonable values of eccentricity in the context of our model. The distribution of mass ratios in primordial binaries is not well known, but for a number of distributions discussed in the literature (see, e.g., Abt & Levy 1976, 1978, 1985; Abt, Gomez, & Levy 1990; Tout 1991; Duquennoy & Mayor 1991; Garmany, Conti, & Massey 1980), there is greater than a 15% probability of finding an initial mass ratio in the range of 0.8–1.0. Finally, after taking into account that $\sim 50\%$ of all stars are in binary systems, it seems reasonable that $\sim 0.3\%$ of all planetary nebulae should have concentric shell structures during the phase before the nebula is ionized. Of approximately 1500 known PNs, this corresponds to about five such objects.

6. SUMMARY

The illustrative evolutionary results shown in Figure 2 demonstrate how the stellar wind of an AGB star, disturbed periodically by a companion in a wide eccentric orbit, can form an object such as CRL 2688 (the Egg Nebula).

In the proposed scenario, the AGB star has an extended atmosphere that is up to 10 times the stellar radius in size. Because of the eccentricity of the orbit, the Roche lobe of the AGB star periodically shrinks and expands during the orbital period. At some point in its evolution, the radius of the AGB star may grow sufficiently, owing to its core evolution, that the extended atmosphere will overtake the Roche lobe during periastron passages; when this happens, the mass loss from the star is diverted from its isotropic wind to a flow that is concentrated toward the equatorial plane of the system. Thus, around each periastron passage, a deficiency in the isotropic mass flow develops, and these deficiencies form lower density concentric shells in the expanding nebula that is formed by the otherwise continuous wind. This structure is approximately spherically symmetric, but with two significant deviations from symmetry. First, there should be excess matter distributed in the orbital plane; this is the matter that is periodically diverted from its spherical outflow. Second, at least in the case of CRL 2688, the nebula is illuminated by the central star, but because of the special way in which it is illuminated, there are substantial enhancements along bipolar jetlike lines. This mechanism is discussed below.

As the evolution proceeds and the stellar radius increases further, the intrusions of the Roche lobe into the extended atmosphere become longer, and toward the end of the evolution they cover more than one-half of the orbital period. By the time the envelope of the AGB star has been completely lost, approximately a few tenths of a solar mass will have been ejected via the superwind into the nebulae that we now observe, at rates up to $\sim 10^{-4}\, M_\odot\ {\rm yr}^{-1}$. In the case of the Egg Nebula, the envelope has either not been completely lost or the mass-loss process is just coming to an end. Hence, the matter in the nebula is still cold, and it shines only as a reflection nebula. Thus, pressure instabilities are not likely to develop, and the shell structure can remain stable for a relatively long time (>1000 yr). When the hot core of the star is eventually exposed, its UV radiation will ionize the surrounding nebula, pressure instabilities will develop, and the ring structure will be destroyed.

The matter diverted from the isotropic flow by the companion star will gather in the equatorial plane and may form a disk surrounding the companion. This disk may have given rise to jets in the polar directions. These jets, which probably became active immediately after the shell-like structure was formed, have not substantially influenced the basic shell structure. However, they have apparently created holes in the dense dust cover that surrounds the star and that otherwise would prevent the stellar radiation from reaching the outer structure (Sahai et al. 1995). As mentioned above, the radiation is allowed through the central dust cover in such a way that the nebula is significantly more illuminated along the jetlike features in the bipolar directions. An analysis of the surface brightness along different directions in the nebula (R. Sahai 1996, private communication) shows that both along the jetlike features and in other directions, the density profile is ringlike. This shows that the underlying shell structure is fairly isotropic and that the asymmetry is largely an illumination effect.

The model described in this work may well lead to the formation of the nebular objects with multiple concentric shells as are observed in the Egg Nebula. However, a specific range of initial binary parameters is needed to form such an object. The most important of these is the existence of a companion star in a modestly eccentric orbit whose distance during the final phases of the PN formation results in the Roche lobe intruding periodically into the extended atmosphere of the AGB star (corresponding to orbital periods of ~ 200 yr). We have estimated that about $\sim 0.3\%$ of all planetary nebulae should have observable concentric ring structure before the nebulae become ionized.

We thank R. Sahai and J. Trauger for allowing us to use some of their *HST* data on the Egg Nebula and for a helpful discussion. As well, we are grateful to P. Eggleton for valuable discussions concerning orbital evolution. This research was supported in part by NASA grant NAG 5-3011.

REFERENCES

Abt, H. A., & Levy, S. G. 1976, ApJS, 30, 273
———. 1978, ApJS, 36, 241
———. 1985, ApJS, 59, 229
Abt, H. A., Gomez, A. E., & Levy, S. G. 1990, ApJS, 74, 551
Alexander, D. R. 1975, ApJS, 29, 363
Avni, Y. 1976, ApJ, 209, 574
Bond, H., & Livio, M. 1990, ApJ, 355, 568
Bowen, G. H. 1988, ApJ, 329, 299
Corradi, R. L. M. 1995, MNRAS, 276, 521
Corradi, R. L. M., & Schwarz, H. E. 1995, A&A, 293, 871
Deguchi, S. 1997, in IAU Symp. 180, Planetary Nebulae, ed. H. Lamers & H. J. Habing, in press
Duquennoy, A., & Mayor, M. 1991, A&A, 248, 485
Eggleton, P. 1966, MNRAS, 132, 479

Eggleton, P. 1997, Evolutionary Processes in Binary and Mutiple Stars, (Cambridge: Cambridge Univ. Press), in preparation
Fabian, A. C., & Hansen, C. J. 1979, 187, 283
Garmany, C. D., Conti, P. S., & Massey, P. 1980, ApJ, 242, 1063
Gilman, R. C. 1972, ApJ, 178, 423
Han, Z., Podsiadlowski, P., & Eggleton, P. 1995, in Asymmetrical Planetary Nebulae, ed. A. Harpaz & N. Soker (Ann. of the Israel Physical Society, Vol. 11) (Bristol: Inst. of Physics Pub.), 66
Hearn, A. G. 1990, in From Miras to Planetary Nebulae, ed. M. O. Mennessier & A. Omont (Paris: Editions Frontières), 121
Iben, I., & Renzini, A. 1983, ARA&A, 21, 271
Johnson, H. R., Alexander, D. R., & Bowen, G. H. 1995, in Asymmetrical Planetary Nebulae, ed. A. Harpaz & N. Soker (Ann. of the Israel Physical Society, Vol. 11) (Bristol: Inst. of Physics Pub.), 98
Joss, P. C., Rappaport, S., & Lewis, W. 1987, ApJ, 319, 180
Kippenhahn, R., Kohl, K., & Weigert, A. 1967, Z. Phys., 66, 58
Knapp, G. R., & Morris, M. 1985, ApJ, 292, 640
Kopal, Z. 1959, Close Binary Systems, (London: Chapmann & Hall)
Kwok, S., Purton, C. R., & FitzGerald, M. P. 1978, ApJ, 219, L125
Latter, W. B., Hora, J. L., Kelly, D. M., Deutsch, L. K., & Maloney, P. R. 1993, AJ, 106, 260
Livio, M. 1982, A&A, 105, 37
Livio, M., Salzman, S., & Shaviv, G. 1979, MNRAS, 188, 1
Morris, M. 1981, ApJ, 249, 572
———. 1987, PASP, 99, 1115
Paczyński, B. 1967a, Acta Astron., 17, 287
———. 1967b, Acta Astron., 17, 193
———. 1970, Acta Astron., 20, 47
Rappaport, S., Podsiadlowski, P., Joss, P. C., DiStefano, R., & Han, Z. 1995, MNRAS, 273, 71
Refsdal, S., & Weigert, A. 1970, A&A, 6, 426
———. 1971, A&A, 13, 367
Reimers, D. 1975, Mem. Soc. R. Sci. Liège, 6th Ser., 8, 369
Renzini, A. 1981, in Physical Processes in Red Giants, ed. I. Iben & A. Renzini (Dordrecht: Reidel), 431
Sahai, R., & Trauger, J. T. 1996, S&T, 91(5), 12
Sahai, R., Trauger, J. T., & Evans, R. W. 1995, BAAS, 187, 4403
Schwarz, H. E., & Corradi, R. L. M. 1995, in Asymmetrical Planetary Nebulae, ed. A. Harpaz & N. Soker (Ann. of the Israel Physical Society, Vol. 11) (Bristol: Inst. of Physics Pub.), 113
Soker, N. 1997, ApJS, in press
Soker, N., & Livio, M. 1994, ApJ, 421, 219
Stanghellini, L. 1995, in Asymmetrical Planetary Nebulae, ed. A. Harpaz & N. Soker (Ann. of the Israel Physical Society, Vol. 11) (Bristol: Inst. of Physics Pub.), 17
Tout, C. A. 1991, MNRAS, 250, 701
Tuchman, Y. 1991, ApJ, 383, 779
Vassiliadis, E., & Wood, P. R. 1993, ApJ, 413, 641
Verbunt, F., & Phinney, E. S. 1995, A&A, 296, 709
Webbink, R. F. 1979a, in IAU Colloq. 46, Changing Trends in Variable Star Research, ed. F. M. Bateson, I. H. Urch, & J. Smak (Hamilton, New Zealand: Univ. of Waikato), 102
———. 1979b, in IAU Colloq. 53, White Dwarfs and Variable Degenerate Stars, ed. H. Van Horn & V. Weidemann (Rochester: Univ. of Rochester Press), 426
———. 1992, in X-Ray Binaries and Recycled Pulsars, ed. E. P. J. van den Heuvel & S. Rappaport (Dordrecht: Kluwer), 269
Webbink, R. F., Rappaport, S., & Savonije, G. J. 1983, ApJ, 270, 678
Wood, P. R. 1986, in Stellar Pulsation, ed. A. N. Cox, W. M. Sparks, & S. G. Starrfield (Berlin: Springer), 250
Yungelson, L. R., Tutukov, A. V., & Livio, M. 1993, ApJ, 418, 794
Zahn, J.-P. 1977, A&A, 57, 383 (erratum A&A, 67, 162 [1978])
———. 1989, A&A, 220, 112